International Journal of Modern Communication Technologies & Research (IJMCTR)
ISSN: 2321-0850, Volume-4, Issue-10, October 2016

A review of saliency-based soft sensors for permanent magnet synchronous machines

Ines Omrane

Abstract— **This paper presents a review of the saliency-based soft sensors. In particular estimator based on rotating or alternating carrier signal injection and methods based on inductance variations, like INFORM, are presented. The soft sensors structure and their design are discussed.**

Index Terms— **Low speed region, Permanent magnet synchronous motor, Sensorless control, Signal injection.**

I. INTRODUCTION

Permanent magnet synchronous machine (PMSM) drive have been increasingly applied in a wide variety of industrial applications by replacing classic dc drives. The reason comes from the special advantages of PMSM such as inherent high power density, high efficiency, simple structure and absence of filed losses. To achieve high performance field-oriented control, accurate rotor position information, which is usually measured by rotary encoders is necessary. However, the cost of a sensor may exceed the cost of a small motor in some applications. Also, the presence of the mechanical sensors not only increases the cost and complexity of the total material with additional wiring but also reduces its reliability with additional sensitivity to external disturbances. In addition, it may be difficult to install and maintain a position sensor due to the limited space and rigid work environment with high vibration or high temperature. Therefore, the idea is to replace the mechanical sensor by a soft sensor which offers a number of attractive properties one of them being a low cost alternative to hardware speed measurement used in classical motor drives [1–3].

During the years, researchers have developed different sensorless techniques. These methods were classified under two main categories:

- Methods suitable for standstill and low speed region,
- Methods adequate for high speed region.

At high speed, the position can be estimated from the first harmonic of the back-emf or from the mathematical model of the drive. Several techniques inspired from control theory [4–6], such as adaptive observers [7–10], reference models [11–13], and extended Kalman filter [14].

At standstill, the PMSM is unobservable since the back-emf are zero. Therefore, classical methods based on the fundamental wave of the back-emf fail in this region.

At low speed, the rotor position can be estimated by using inductance variations due to magnetic saturation and/or geometrical effects of PMSM. This is achieved by injecting a high frequency signal in the stator windings of the main generator. This signal can be a voltage or a current signal, having a frequency other than the fundamental. Correspondingly, the current or the voltage response, containing information on the anisotropy, can be used for detecting the rotor position.

The injection of HF currents presents some drawbacks such as the bandwidth estimation is limited by the current controller bandwidth. This problem disappears when a voltage is injected. In this case, the estimation bandwidth is determined by the observer bandwidth.

Several techniques have been developed in order to offer a solution to the estimation problems at low speeds. Thus, the startup of the motor can be provided in a closed loop. In this paper, the principle of the most popular sensorless techniques is presented.

Ines Omrane, University of Poitiers, Laboratoire d'Informatique et d'Automatique pour les Systèmes, Poitiers, France.

II. INFORM METHOD

The INFORM method " INdirect Flux detection by Online Reactance Measurement" was first introduced by Shroedl [15]. This method was based on real-time inductance measurements using saliency and saturation effects. A sequence of discrete voltage pulses is injected into the machine, and the rotor position estimate is deduced from the difference in the stator inductance.

The stator voltage and stator flux linkage equations in space phasors can be described in the following way:

$$u_s = R_s\, i_s + \frac{d\psi_s}{dt} \qquad (1)$$
$$\psi_s = L_s\, i_s + \psi_{pm}$$

For a sufficiently high frequency of injection, it can be considered that the stator resistance impedance is negligible compared to the inductances impedances. Furthermore a measurement at standstill induced no back-emf. With this assumption the complex INFORM inductance can be defined [15]:

$$L_{INFORM} = \frac{u_s}{{d i_s}/{dt}} \qquad (2)$$

where L_{INFORM} is the complex INFORM reactance, i_s is the complex stator current and t is the time.

The current change with respect to the voltage depends on the rotor position. In [16], the authors propose to calculate the incremental inductance in real time and then to deduce the rotor position. This inductance can be given by equation (3) by neglecting the emf at standstill or low speed.

$$L(i,\theta) = \frac{u_s - R_s i_s}{\frac{di_s}{dt}} \tag{3}$$

We note that the inductance can be calculated from the voltage and the measured current. Furthermore, it can be written as follows

$$L(i,\theta) = L_0(i) + L_1(i)\cos(\theta) + L_2(i)\cos(2\theta) \tag{4}$$

Equation (4) represents the first three terms of the Fourier series. By identifying the equations (3) and (4) and using a correspondence relationship between the inductance, the current and position, we can estimate the rotor position.

In the INFORM method, the current variations caused by the injection voltages are directly used for estimating the rotor position. The machine parameters will not be involved in the calculation. Therefore, the INFORM method is one kind of parameter independent sensorless control method. However, the main drawback with INFORM is the unsatisfactory accuracy since current variations are the only variables used for the estimation. Therefore, the performance of the position estimation can be dramatically affected by the accuracy of the injected voltage vectors on the machine terminals.

III. Current impulses method

This method It is based on the injection of voltage pulses in the motor phases and the measurement of the related current peeks. The impulses imposed must be sufficiently large to produce a change in the saturation state of the engine. When a voltage step is applied to the phase 'a', the current response can be written as:

$$i_a = \frac{u_a}{R_s}\left(1 - e^{\frac{R_s t}{L_a(\theta)}}\right) \tag{5}$$

By applying positive and negative voltage pulses on phase 'a', the related currents i^+_a and i^-_a can be measured respectively. The rotor position is then determined from the difference between these two peaks. For positive impulse, the stator flux is in the same direction as with the mutual flux. Therefore, the total flux ψ_a can be given by

$$\psi_a = \psi_{am} + \psi_{aa} \tag{6}$$

While for a negative impulse of same duration, the stator flux is in the opposite direction of the mutual flux and consequently the resulting total flux can be written as

$$\psi_a = \psi_{am} - \psi_{aa} \tag{7}$$

Therefore, the saturation is lower compared to the case of a positive impulse. The difference of amplitude between the two current peaks allows to calculate the half of the electrical period, thus the rotor position. The same technique is applied to the phase 'b'.

The current differences Δi_a and Δi_b can be written as follows

$$\Delta i_a = i^+_a - |i^-_a|$$
$$\Delta i_b = i^+_b - |i^-_b| \tag{8}$$

Since Δi_a and Δi_b vary in a sinusoidal way for the different rotor positions, then the estimated position can be obtained by simple trigonometric calculations.

This technique has been used in several publications [17–18], and it was considered as a simple method allowing the discriminate between a north and a south pole of the machine. However, the current impulses injection generates a large amount of noise which must be reduced in order to obtain a good accuracy.

IV. High frequency Signal injection

The high frequency method for estimating the rotor position was a hot research topic due to improvements in power technologies. This method exploits the different anisotropies of the machine, such as magnetic saliency, saturation and eddy current to detect the rotor position. This method has the same principle as a mechanical sensor. It is based on the injection of a high frequency voltage (or current). The measured current (or voltage) contains information about the rotor position. Different types of high frequency signals can be injected. the most used ones are the rotating high frequency signal and the pulsating high frequency signal.

The magnitude of the injected signal should be selected such that the rotor remains at standstill during the estimation phase. The frequency of this signal may vary between *100 Hz* and *4KHz*. The most used frequency is *500Hz*.

A. Rotating high frequency carrier injection

In 1995, the rotating voltage injection has been tested on the interior PMSM [19]. Many saliencies have been exploited to extract the rotor position. Generally the injected signal is a HF balanced three phase voltage (or current) which can be carried by the (α, β) axes [20–22] or the (d, q) axes [23-25]. It has been proved that the current injection requires that the bandwidth of the current regulators must be greater than the injection frequency. Therefore, the injected signal is often a high frequency voltage. The PMSM can be modeled in the *dq* reference frame by the following set of equations

$$\begin{bmatrix} u_d \\ u_q \end{bmatrix} = \begin{bmatrix} R_s & 0 \\ 0 & R_s \end{bmatrix}\begin{bmatrix} i_d \\ i_q \end{bmatrix} + \begin{bmatrix} \frac{d}{dt} & -\omega_e \\ \omega_e & \frac{d}{dt} \end{bmatrix}\begin{bmatrix} \psi_d \\ \psi_q \end{bmatrix} \tag{9}$$

where

$$\begin{bmatrix}\psi_d\\ \psi_q\end{bmatrix}=\begin{bmatrix}L_d & 0\\ 0 & L_q\end{bmatrix}\begin{bmatrix}i_d\\ i_q\end{bmatrix}+\begin{bmatrix}\psi_{pm}\\ 0\end{bmatrix} \quad (10)$$

In the fixed reference frame, the PMSM model can be given by

$$\begin{bmatrix}u_\alpha\\ u_\beta\end{bmatrix}=R_s\begin{bmatrix}i_\alpha\\ i_\beta\end{bmatrix}+\frac{d}{dt}\begin{bmatrix}\psi_\alpha\\ \psi_\beta\end{bmatrix} \quad (11)$$

where

$$\begin{bmatrix}\psi_\alpha\\ \psi_\beta\end{bmatrix}=\begin{bmatrix}L_{\alpha\beta}\end{bmatrix}\begin{bmatrix}i_\alpha\\ i_\beta\end{bmatrix}+\psi_{pm}\begin{bmatrix}\cos\theta_e\\ \sin\theta_e\end{bmatrix} \quad (12)$$

Let

$$L_{diff}=\frac{L_q-L_d}{2} \quad (13)$$

and

$$L_{moy}=\frac{L_q+L_d}{2} \quad (14)$$

So we have

$$\begin{bmatrix}L_{\alpha\beta}\end{bmatrix}=\begin{bmatrix}L_{moy}-L_{diff}\cos 2\theta_e & -L_{diff}\sin 2\theta_e\\ -L_{diff}\sin 2\theta_e & L_{moy}+L_{diff}\cos 2\theta_e\end{bmatrix} \quad (15)$$

The injected signal can be given by the following equation where u_i is the magnitude of the injected voltage which should be properly selected, such that the rotor remains stationary upon the injection.

$$\begin{bmatrix}u_{\alpha i}\\ u_{\beta i}\end{bmatrix}=u_i\begin{bmatrix}\cos(\omega_i t)\\ \sin(\omega_i t)\end{bmatrix} \quad (16)$$

Then the stator currents can be given by

$$\begin{bmatrix}i_{\alpha i}\\ i_{\beta i}\end{bmatrix}=u_i\begin{bmatrix}I_{pi}\sin(\omega_i t)+I_{ni}\sin(2\theta_e-\omega_i t)\\ -I_{pi}\cos(\omega_i t)-I_{ni}\cos(2\theta_e-\omega_i t)\end{bmatrix} \quad (17)$$

where I_{pi} and I_{ni} are respectively the direct and the inverse components of the stator currents.
They can be expressed as follows:

$$I_{pi}=\frac{u_i L_{moy}}{\omega_i\left(L_{moy}^2-L_{diff}^2\right)} \quad (18)$$

$$I_{ni}=\frac{u_i L_{diff}}{\omega_i\left(L_{moy}^2-L_{diff}^2\right)} \quad (19)$$

We can note that I_{ni} contains information about the rotor position. In order to extract this information, I_{pi} must be completely eliminated. In [22], Wang proposed the following block diagram given by Fig. 1 where filters and an integral proportional corrector are used for the extraction of the rotor position.

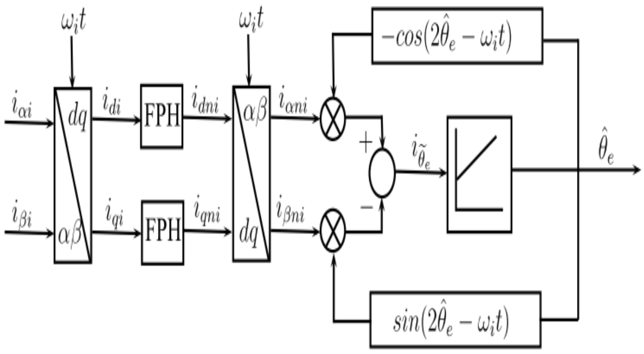

Fig. 1. Block diagram of the rotor position estimation

where $i_{\tilde{\theta}_e}$ is calculated as follows

$$\begin{aligned}i_{\tilde{\theta}_e}&=-i_{\alpha ni}\cos\left(2\hat{\theta}_e-\omega_i t\right)-i_{\beta ni}\sin\left(2\hat{\theta}_e-\omega_i t\right)\\ &=I_{ni}\sin\left(2\left(\hat{\theta}_e-\theta_e\right)\right)=I_{ni}\sin\left(2\tilde{\theta}_e\right)\end{aligned} \quad (20)$$

Then, the estimated rotor position can be given by

$$\hat{\theta}_e=\left(K_p+K_i\int dt\right)i_{\tilde{\theta}_e} \quad (21)$$

B. Pulsating high frequency carrier injection

The pulsating high frequency injection scheme makes also use of the saliencies present in the machine to extract the position. Usually, a HF signal is injected in one axis of the reference frame. If the injected signal is a voltage, then the carrier current response along the axis orthogonal to the injection axis contains the rotor position information.

Therefore, a high frequency voltage is added to the d-axis control output as follows:

$$\begin{bmatrix}u_{di}\\ u_{qi}\end{bmatrix}=u_i\begin{bmatrix}\cos(\omega_i t)\\ 0\end{bmatrix} \quad (22)$$

By injecting a carrier high-frequency signal, the machine can be considered as a RL load given by the following equations:

$$u_{di}=R_s i_{di}+L_d\frac{di_{di}}{dt}=\left(R_s+j\omega_i L_d\right)i_{di}\equiv z_d i_{di} \quad (23)$$

$$u_{qi}=R_s i_{qi}+L_q\frac{di_{qi}}{dt}=\left(R_s+j\omega_i L_q\right)i_{qi}\equiv z_q i_{qi} \quad (24)$$

where u_{di} and u_{qi} are the stator voltages at HF, i_{di} and i_{qi} are the stator currents at HF, z_d and z_q are the d- and q-axes impedances, respectively, ω_i is the frequency of the injected signal.

Equations (23) and (24) may be given by:

$$\begin{bmatrix}u_{di}\\ u_{qi}\end{bmatrix}=\begin{bmatrix}z_d & 0\\ 0 & z_q\end{bmatrix}\begin{bmatrix}i_{di}\\ i_{qi}\end{bmatrix} \quad (25)$$

Since

$$\begin{bmatrix} i_{di} \\ i_{qi} \end{bmatrix} = \begin{bmatrix} \cos\tilde{\theta}_e & \sin\tilde{\theta}_e \\ -\sin\tilde{\theta}_e & \cos\tilde{\theta}_e \end{bmatrix} \begin{bmatrix} \hat{i}_{di} \\ \hat{i}_{qi} \end{bmatrix} \quad (26)$$

Then

$$\hat{i}_{di} = \frac{1}{z_d z_q}\left[\left(\frac{z_d+z_q}{2} - \frac{z_d-z_q}{2}\cos 2\tilde{\theta}_e\right)\hat{u}_{di} - \frac{z_d-z_q}{2}\sin 2\tilde{\theta}_e \hat{u}_{qi}\right] \quad (27)$$

and

$$\hat{i}_{qi} = \frac{1}{z_d z_q}\left[-\frac{z_d-z_q}{2}\sin 2\tilde{\theta}_e \hat{u}_{di} + \left(\frac{z_d+z_q}{2} + \frac{z_d-z_q}{2}\cos 2\tilde{\theta}_e\right)\hat{u}_{qi}\right] \quad (28)$$

Let

$$z_{diff} = z_d - z_q \quad (29)$$

and

$$z_{moy} = \frac{z_q + z_d}{2} \quad (30)$$

Then

$$\hat{i}_{di} = \frac{1}{z_d z_q}\left[\left(z_{moy} - \frac{1}{2} z_{diff}\cos 2\tilde{\theta}_e\right)\hat{u}_{di} - \frac{1}{2} z_{diff}\sin 2\tilde{\theta}_e \hat{u}_{qi}\right] \quad (31)$$

and

$$\hat{i}_{qi} = \frac{1}{z_d z_q}\left[-\frac{1}{2} z_{diff}\sin 2\tilde{\theta}_e \hat{u}_{di} + \left(z_{moy} + \frac{1}{2} z_{diff}\cos 2\tilde{\theta}_e\right)\hat{u}_{qi}\right] \quad (32)$$

The carrier current response along the q-axis is then given by:

$$\hat{i}_{qi} = \frac{-u_i \sin 2\tilde{\theta}_e}{2\omega_i L_d L_q}\left(z_{diff}\sin \omega_i t\right) \quad (33)$$

For a sufficiently high frequency of injection, it can be considered that the stator resistance impedance is negligible compared to the inductances impedances

$$\begin{aligned} z_d &= R_s + j\omega_i L_d \equiv j\omega_i L_d \\ z_q &= R_s + j\omega_i L_q \equiv j\omega_i L_q \\ z_{diff} &= j\omega_i L_{diff} = j\omega_i\left(L_d - L_q\right) \end{aligned} \quad (34)$$

Then, $\hat{i}_{qi}$ can be written by:

$$\hat{i}_{qi} = \frac{-u_i \sin 2\tilde{\theta}_e}{2\omega_i L_d L_q}\left(L_{diff}\sin \omega_i t\right) \quad (35)$$

$\hat{i}_{qi}$ depends on the position error $\tilde{\theta}_e$, so a synchronous demodulation is required to calculate the proportional signal to the estimation error of the rotor position. The use of analog filters allows the isolation of the term that contains information about the position and the elimination of undesirable terms. In general, the diagram can be given by Fig.2. The band pass filter (BPF) is centered on the carrier frequency. The resulting current is then multiplied by $\sin(\omega_i t)$. At the end, a low pass filter is used to get back the signal $i_{\tilde{\theta}_e}$ approached by equation (36)

$$i_{\tilde{\theta}_e} \equiv LPF\left(\hat{i}_{qi}\sin\omega_i t\right) = \frac{-u_i L_{diff}}{4\omega_i L_d L_q}\sin 2\tilde{\theta}_e \quad (36)$$

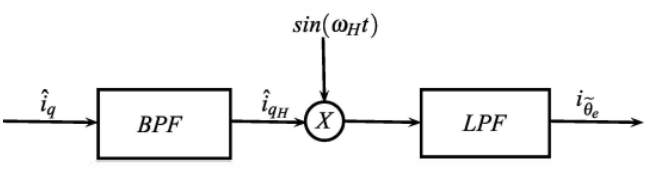

Fig. 2. Demodulation scheme used to obtain the position error signal

Suppose that the rotor position estimation error is so small ($\sin 2\tilde{\theta}_e \approx 2\tilde{\theta}_e$). Then,

$$i_{\tilde{\theta}_e} \approx \frac{-u_i L_{diff}}{2\omega_i L_d L_q}\tilde{\theta}_e \quad (37)$$

Finally, the rotor speed can be estimated using a PI controller

$$\hat{\omega}_e = \chi_p i_{\tilde{\theta}_e} + \chi_i \int i_{\tilde{\theta}_e} dt \quad (38)$$

where χ_p and χ_i are proportional and integral gain of the controller. The rotor position estimate is given by:

$$\hat{\theta}_e = \int \hat{\omega}_e dt \quad (39)$$

V. Simulation Results

In this section we present the simulation results of a soft sensor based on signal injection technique. We inject a HF alternative voltage. Indeed, this method was more accurate. Fig. 3 shows the simulation results where (a) actual and estimated mechanical speed, (b) actual and estimated electric position, (c) speed estimation error, (d) position estimation error. This soft sensor provides a good estimate of the speed and position of the MSAP at low speed and even at a standstill.

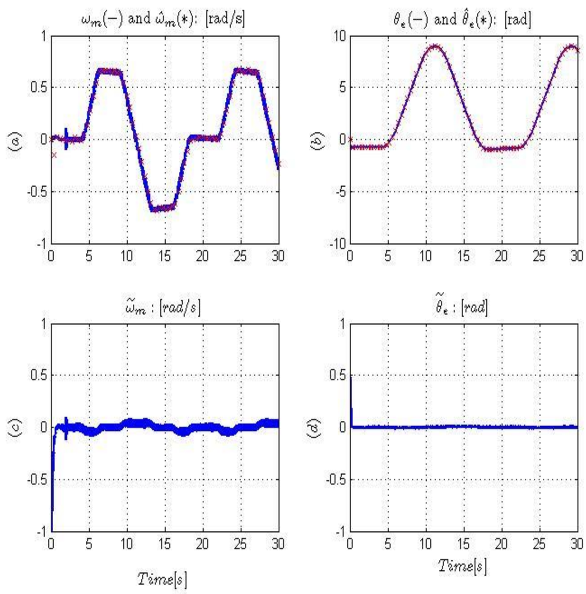

VI. CONCLUSION

In this paper, most of the used sensorless techniques have been described for standstill and low speed. The position estimation method based on the injection of a rotating or a pulsating high frequency signal is presented. The basics of the scheme, the used filtering and the observer structure are shown. The INFORM method based on inductance variations, is also presented.

REFERENCES

[1] R. Abdelli, D. Rekioua, T. Rekioua (2011), "Performances improvements and torque ripple minimization for VSI fed induction machine with direct control torque". *ISA Trans*, Vol. 50, Iss. 2, pp. 213-219.

[2] A.Y. Achour, B.Mendil, S. Bacha, I. Munteanu (2009), "Passivity-based current controller design for a permanent-magnet synchronous motor". *ISA Trans*, Vol. 48, Iss. 3, pp. 336-346.

[3] B. Zhang, Y. Pi, Y. Luo (2012), "Fractional order sliding-mode control based on parameters auto-tuning for velocity control of permanent magnet synchronous motor". *ISA Trans*, Vol. 51, Iss. 5, pp. 649-656.

[4] Ph. Bogaerts, A. VandeWouwer (2003). "Software sensors for bioprocesses". *ISA Trans*, Vol. 42, Iss. 4, p.p. 547-558.

[5] R. F. Escobar, C. M. Astorga-Zaragoza, A. C. Tellez-Anguiano, D. Juarez-Romero, J. A. Hernandez, G. V. Guerrero-Ramirez (2011). "Sensor fault detection and isolation via high-gain observers: application to a double-pipe heat exchanger". *ISA Trans*, Vol. 50, Iss. 3, p.p. 480-486.

[6] S. R. Vijaya Raghavan, T. K. Radha krishnan, K. Srinivasan (2011). "Soft sensor based composition estimation and controller design for an ideal reactive distillation column". *ISA Trans*, Vol. 50, Iss. 1, p.p. 61-70.

[7] H. Kubota, K. Matsuse (1993). "DSP-based speed adaptive flux observer of induction motor". *IEEE Trans Ind Appl*, Vol. 29, Iss. 2, p.p. 344–348.

[8] H. R. Karimia, A. Babazadehb (2005). "Modeling and output tracking of transverse flux permanent magnet machines using high gain observer and RBF neural network". *ISA Trans*, Vol. 44, Iss. 4, p.p. 445-456.

[9] M. Hinkkanen, M. Harnefors, J. Luomi (2010). "Reduced-order flux observers with stator-resistance adaptation for speed-sensorless induction motor drives". *IEEE Trans Power Electron*, Vol. 25, Iss. 5, p.p. 1173-1183.

[10] S. Zheng, X. Tang, B. Song, S. Lu, B. Ye (2013). "Stable adaptive PI control for permanent magnet synchronous motor drive based on improved JITL technique". *ISA Trans*, Vol. 52, Iss. 4, p.p. 539-549.

[11] G. Yang, T. Chin (1993). "Adaptive-Speed identification scheme for a vector-controlled speed sensorless inverter-induction motor drive". *IEEE Trans Ind Appl*, Vol. 29, Iss. 4, p.p. 820-825.

[12] G. Madadi-Kojabadi (2005). "Simulation and experimental studies of model reference adaptive system for sensorless induction motor drive". *Simul Model Pract Theory*, Vol. 13, Iss. 6, p.p. 451-464.

[13] T. Orlowska-Kowalska, M. Dybkowski (2010). "Stator-current-based MRAS estimator for a wide range speed-sensorless induction-motor drive". *IEEE Trans Ind Electron*, Vol. 57, Iss. 4, p.p. 1296-1308.

[14] D. Xu, S. Zhang, J. Liu (2013). "Very-low speed control of PMSM based on EKF estimation with closed loop optimized parameters". *ISA Trans*, Vol. 52, Iss. 6, p.p. 835-843.

[15] M. Schroedl (1996). "Sensorless control of AC machines at low speed and standstill based on the INFORM method". Industry Applications Conference IEEE-IAS Annual Meeting, Vol. 1, p.p. 270-277.

[16] H. Gao, F.R. Salmasi, M. Ehsani (2004). "Inductance model-based sensorless control of the switched reluctance motor drive at low speed". *IEEE Trans Power Electron*, Vol. 19, Iss. 6, p.p. 1568-1573.

[17] M. Boussak (2005). "Implementation and experimental investigation of sensorless speed control with initial rotor position estimation for interior permanent magnet synchronous motor drive". *IEEE Trans Power Electron*, Vol. 20, Iss. 6, pp. 1413-1422.

[18] M. Tursini, R. Petrella, F. Parasiliti (2003). "Initial rotor position estimation method for PM motors". *IEEE Trans. Ind. Appl*, Vol. 39, Iss. 6, pp. 1630-1640.

[19] P. L. Jansen, M. J. Corley, R. D. Lorenz (1995). "Flux, position, and velocity estimation in AC machines at zero and low speed via tracking of high frequency saliencies". European Conference on Power Electronics and Applications EPE, Sevilla, Spain, p.p. 154-160.

[20] D. Saltiveri, A. Arias, G. Asher, M. Sumner, P. Wheeler, L. Empringham, C. Silva (2006). "Sensorless control of surface-mounted permanent magnet synchronous motors using matrix converters". *Electrical Power Quality and Utilization, Journal EPQU*, Vol. 12, Iss.1, pp. 59- 67.

[21] O. Mansouri-Toudert, H. Zeroug, F. Auger, A. Chibah (2012). "Improved rotor position estimation of salient-pole PMSM using high frequency carrier signal injection". International Conference on Electrical Machines ICEM, Marseille, France, p.p. 761-767.

[22] G. Wang, R. Yang, Y. Wang, Y. Yu, D. Xu (2010). "Initial rotor position estimation for sensorless interior PMSM with signal injection". International Power Electronics Conference IPEC, pp. 2748-2752.

[23] M. Linke, R. Kennel, J. Holtz (2002). "Sensorless position control of permanent magnet synchronous machines without limitation at zero speed". The 28th annual conference of the IEEE industrial electronics society IECON, Sevilla, Spain, p.p. 674-679.

[24] S. Kim, S. K. Sul (2011). "High performance position sensorless control using rotating voltage signal injection in IPMSM". The 14th European Conference on Power Electronics and Applications EPE.

[25] Y. Jeong, R. D. Lorenz, T. M. Jahns, S. Sul (2003). "Initial rotor position estimation of an interior permanent magnet synchronous machine using carrier-frequency injection methods". IEEE International Electric Machines and Drives Conference IEMDC.